

# Formulation and Biomedical Activity of Oil-in-Water Nanoemulsion Combining *Tinospora smilacina* Water Extract and *Calophyllum inophyllum* Seeds Oil

Elnaz Saki<sup>1</sup>, Vinuthaa Murthy<sup>1</sup>, Hao Wang<sup>1</sup>, Roshanak Khandanlou<sup>1</sup>, Johanna Wapling<sup>2</sup>, Richard Weir<sup>3</sup>

<sup>1</sup>Faculty of Science and Technology, Charles Darwin University, Darwin, Northern Territory, Australia; <sup>2</sup>Menzies School of Health Research, Charles Darwin University, Darwin, Northern Territory, Australia; <sup>3</sup>Department of Industry, Tourism and Trade, Berrimah Veterinary Laboratory, Darwin, Northern Territory, Australia

Correspondence: Elnaz Saki, Faculty of Science and Technology, Charles Darwin University, Darwin, Northern Territory, 0909, Australia, Tel +61 42439 3238, Email elnaz.saki@cdu.edu.au

**Introduction:** *Tinospora smilacina* is a native plant used in traditional medicine by First Nations peoples in Australia to treat inflammation. In our previous study, an optimised *Calophyllum inophyllum* seed oil (CSO) nanoemulsion (NE) showed improved biomedical activities such as antimicrobial, antioxidant activity, cell viability and in vitro wound healing efficacy compared to CSO.

**Methods:** In this study, a stable NE formulation combining *T. smilacina* water extract (TSWE) and CSO in a nanoemulsion (CTNE) was prepared to integrate the bioactive compounds in both native plants and improve wound healing efficacy. D-optimal mixture design was used to optimise the physicochemical characteristics of the CTNE, including droplet size and polydispersity index (PDI). Cell viability and in vitro wound healing studies were done in the presence of CTNE, TSWE and CSO against a clone of baby hamster kidney fibroblasts (BHK-21 cell clone BSR-T7/5).

**Results:** The optimised CTNE had a  $24 \pm 5$  nm particle size and  $0.21 \pm 0.02$  PDI value and was stable after four weeks each at 4 °C and room temperature. According to the results, incorporating TSWE into CTNE improved its antioxidant activity, cell viability, and ability to promote wound healing. The study also revealed that TSWE has >6% higher antioxidant activity than CSO. While CTNE did not significantly impact mammalian cell viability, it exhibited wound-healing properties in the BSR cell line during in vitro testing. These findings suggest that adding TSWE may enhance CTNE's potential as a wound-healing treatment.

**Conclusion:** This is the first study demonstrating NE formulation in which two different plant extracts were used in the aqueous and oil phases with improved biomedical activities.

**Keywords:** medicinal plants, nanoemulsion, RSM, wound healing, in vitro

## Introduction

There has been a significant advancement in natural remedies with healing potential for skin cuts, burns, and wounds.<sup>1,2</sup> However, wound healing is amongst the most complicated processes in the human body. The skin presents an efficient barrier to protect the body from the penetration of molecules and microorganisms in the external atmosphere and extreme water loss to maintain homeostasis.<sup>3</sup> The difficulty of effective administration to the target site has been identified as a significant challenge in the pharmaceutical industry.<sup>4,5</sup> Nanosystems can be designed to interact with the outermost layer of skin, the stratum corneum (SC), which is a barrier to the penetration of many substances. By incorporating specific properties such as small particle size, surface charge, and hydrophobicity, nanosystems can penetrate the SC and reach deeper skin layers or tissues.<sup>6</sup> Nanoemulsions (NE) are an emerging class of nanosystems that have shown great potential in improving therapeutic effectiveness.<sup>7</sup>

NEs are stable colloidal systems of oil and water, stabilised by surfactants.<sup>5</sup> Maintaining the elements and characteristics of the NE formulation to achieve optimal bioavailability and minimal skin irritation plays an important role.<sup>8</sup> Certain factors, including polarity, volatility, solubility, and the presence of organic solvents of the active compound need

to be considered to select the nanosystem.<sup>5,9</sup> Depending on the extraction method, plant extracts can possess many active molecules, such as phenolic compounds.<sup>10</sup>

In our previous work,<sup>11</sup> we formulated a NE containing *Calophyllum inophyllum* L. (Clusiaceae) (CSONE) as cold-pressed seed oil (CSO). The CSONE was stable and enhanced biomedical properties including antioxidant activity, cell viability, in vitro wound healing, and antimicrobial activity compared to the CSO.<sup>11</sup> In this investigation, we introduced a plant-based water component to the NE in an effort to enhance the properties of the plant-based oil NE.

For this study, *Tinospora smilacina* water extract (TSWE) and *Calophyllum inophyllum* L. (Clusiaceae), cold-pressed seed oil, were used to formulate stable NE. *Tinospora smilacina* Benth. (Menispermaceae), commonly known as “snakevine”, is a semi-deciduous woody, creeping vine plant found in northern New South Wales and central Northern Australia.<sup>12</sup> The stems, leaves, and roots have been used as traditional medicines by Australian First Nations peoples to treat inflammatory disorders such as swelling, wound infection, colds and snake bite<sup>13,14</sup> and to cover boils.<sup>15</sup> Long-chain unsaturated fatty acids<sup>16</sup> and alkaloids<sup>15</sup> were identified in this species which may be responsible for exhibiting diverse biological activities, such as those that are antimalarial,<sup>17</sup> anti-inflammatory, and wound healing.<sup>18</sup> However, there is a lack of published data on the wound healing properties and cytotoxic effects of *T. smilacina*. In addition, studies on *C. inophyllum* seeds, bark and leaf extracts have shown potential pharmaceutical value, with antioxidant, antimicrobial, antiproliferative, antitumor, and anti-inflammatory activities.<sup>19–24</sup>

The current study describes the generation of a stable NE combining TTSWE as with CSO, following the Response Surface Methodology (RSM) design. Encapsulating these two agents into one NE was expected to retain the properties of the biologically active ingredients. The optimum formulation and fabrication parameters for designing the NE need to be appropriately assessed in order to achieve a NE with desirable stability. The conventional experimental approach for optimising parameters can be costly and time-consuming. Hence, numerical methods such as RSM can reduce the experimental parameters of conventional experimentation.<sup>25,26</sup> Using mathematical models and statistical techniques, RSM can investigate the relationship and interaction of independent variables with the response variables. The mixture design statistical method is the most suitable design for optimising pharmaceutical formulations, such as gel and tablets.<sup>27,28</sup> In this study, the D-optimal mixture design was used as it has a smaller number of runs and thus lowers the cost of experimentation.<sup>29</sup> The stability and bioactivity of NE optimised were evaluated and compared with CSONE, CSO and TSWE.

## Methodology

### Materials and Reagents

*T. smilacina* (TS) leaves were collected By Elnaz Saki and Dr Penny Wurm from the Charles Darwin University campus, Ellengowan Dr, Casuarina, NT, 0810 (12°22'12" S, 130° 52' 2" E) vouchered by specimen Saki 1 and the collections were authenticated by Dr Penny Wurm. The voucher specimen is deposited at the Northern Territory Herbarium in Darwin, NT (D0289936). *Calophyllum inophyllum* seed oil (CSO) was purchased from Tamanu NT, a company based in Darwin, Northern Territory (NT), Australia, that produces CSO in bulk by cold press method from seeds collected in the Darwin region. Polysorbate 80 (Tween 80) (P6224), sodium methoxide (S0485), n-hexane (270504), 3-(4,5-dimethylthiazol-2-yl)-2,5-diphenyl tetrazolium bromide (MTT) (M2128) and dimethyl sulfoxide (DMSO) (D8418) were purchased from Sigma Aldrich, Australia and 2,2-diphenyl-1-picryl-hydrazyl (DPPH) (ALF044150), butylated hydroxytoluene (BHT) (ACR11299) were purchased from Thermo Fisher Scientific, Australia. The baby hamster kidney clone BHK-21 (BSR) cell line was kindly provided by the Berrimah Veterinary Laboratory, Northern Territory, Australia.

### Extraction of *Tinospora smilacina* Leaves

The extraction protocol for TS leaves was optimised to obtain the highest chromatogram peaks obtained on the liquid chromatography–mass spectrometry (LC–MS). The optimal extraction method for TS leaf water extract (TSWE) was prepared from fresh TS leaves dried at 60 °C for six hours. After the dried leaves were cooled to room temperature, they were ground to a fine powder with the Laboratory Rotor Mill Pulverisette 14 (LAVAL LAB, North America). Powdered leaf (5.0 g) was mixed with 100 mL boiling high pure water (HPW) for five minutes and shaken for six hours using an

orbital shaker (BIOBASE, China) at room temperature of  $25 \pm 1$  °C. The liquid extract was separated from the solids by filtration with cloth and then filter paper (Whatman, 12 mm) with suction. The extract was transferred to sterile falcon 50 mL high-clarity polypropylene (PP) tubes (Sigma-Aldrich, Australia) and stored at  $-20$  °C for further use.

## Liquid Chromatography–Mass Spectrometry Analysis of TSWE

The TSWE was analysed with an LC-QTOF/MS system (Agilent Technologies), consisting of a 1260 LC coupled to a 6530 QTOF-MS equipped with an electrospray ionisation source. LC separation was accomplished on a Zorbax Eclipse plus C18 column ( $2.1 \times 50$  mm,  $1.9 \mu\text{m}$ ) at  $35$  °C. The injection volume was  $2.0 \mu\text{L}$ . The mobile phases consist of solution A 0.1% v/v formic acid in water and solution B 0.1% formic acid in acetonitrile. The MS was tuned for a low mass range (up to 1700 m/z) and run positive mode for a full scan. Data were collected and processed using “MassHunter” B.05.00 Service Pack 3.

## Preparation of CTNE

The CTNE containing TSWE and CSO was prepared by mixing dispersed and continuous phases. The dispersed phase was prepared by dissolving CSO in Tween 80 as a surfactant. The continuous phase was an aqueous phase consisting of an equal amount of HPW and TSWE. The coarse oil-in-water (o/w) emulsion was prepared by mixing the oil and water phases at 200–300 rpm for 15 min at  $40$  °C using an overhead stirrer. The coarse emulsion was then homogenised at 20,000 rpm for 20 min using a high shear homogeniser (IKA T18 Ultra-Turrax, Germany). The temperature was controlled ( $40^\circ\text{C} \pm 2^\circ\text{C}$ ) by placing the emulsion in an ice bath during homogenisation. The final CTNE was divided into two sterile falcon 50 mL tubes and stored at room temperature and  $4$  °C for stability analysis.

## Characterisation of CTNE

The characterisation of NE has been described in a previous study.<sup>11</sup> Briefly, particle size and PDI values of the NEs were evaluated using dynamic light scattering (DLS) measurements, and the morphology was examined using TEM (JEM-1400, JEOL Co., Japan).

## Optimisation of CTNE by Response Surface Methodology and Statistical Analysis

NE formulation was optimised using a D-optimal mixture design (DMD). Fourteen runs were generated using Design-Expert® 12 software (Stat ease Inc., Minneapolis, USA). The DMD was constructed to minimise the overall variance of the predicted regression coefficient by maximising the value of the determinant of the information matrix.<sup>30</sup> The DMD was used to study the effects of the independent variables: CSO ( $X_1$ ), Tween 80 ( $X_2$ ), HPW: TSWE (1:1) ( $X_3$ ) on the responses: droplet size and PDI and CTNE. The current design evaluated three mixture components (Table 1) by changing individual concentrations and keeping their total 100.

$$X_1 + X_2 + X_3 = 100\% \quad (1)$$

A nonlinear response function was required for constructing the final model. The RSM presents crucial knowledge on the impact of variables and responses of interest with the smallest number of experiments. A second-order quadratic equation was used to express the responses: droplet size and PDI of CTNE as a function of the independent variables as follows:

**Table 1** Mixture Components Values Used in D-Optimal Mixture Design (DMD)

Component	Name	Units	Type	Minimum	Maximum	Coded Low	Coded High
A	CSO	%	Mixture	6	8	+0 ↔ 6	+0.25 ↔ 8
B	Tween 80	%	Mixture	18	24	+0 ↔ 18	+0.75 ↔ 24
C	TSWE: HPW	%	Mixture	68	76	+0 ↔ 68	+1 ↔ 76
				<b>Total = 100</b>			

**Abbreviations:** CSO, *Calophyllum inophyllum* seed oil; HPW, high pure water; TSWE, *Tinospora smilacina* water extract.

$$Y = \beta_0 + \sum_{i=1}^k \beta_i X_i + \sum_{i=1}^k \beta_{ii} X_i^2 + \sum_{i=1}^k \sum_{j=1}^k \beta_{ij} X_{ij} X_{ji} + \varepsilon \quad (2)$$

Equation 2 models the response  $Y$  with the factors of independent variables  $X$ . This model incorporates the models of complex orders, where  $k$  represents the total number of patterns of a particular order and  $i$  and  $j$  represent individual patterns. The coefficients for various orders are referred to as  $\beta$ , where  $\beta_{ij}$  represents the interaction effect,  $\beta_{ii}$  the quadratic effect, and  $\beta_0$  represents the final adjustment constant. The error between the observed and predicted values is represented by the term  $\varepsilon$  in the model.<sup>31</sup>

## Cell Viability Assay

Cell viability in the presence of CTNE, TSWE and CSO against BHK-derived cell line (BSR T7/5),<sup>32</sup> was determined using the 3-(4,5-dimethylthiazol-2-yl)-2,5-diphenyl tetrazolium bromide (MTT) assay (211).<sup>33</sup> The cell viability method was described in our previous study.<sup>11</sup> The CTNE concentration range tested was 60–4000  $\mu\text{g/mL}$ . The CSO and TSWE were tested at the same concentration range as in CTNE, 2.18–70  $\mu\text{g/mL}$  and 22.5–720  $\mu\text{g/mL}$ , respectively. A CSO stock solution was prepared by mixing CSO with DMSO in a 1:3 ratio, then diluted with HPW. The TSWE was also diluted with HPW. The DMSO (0.07–1.12  $\mu\text{g/mL}$ ) and Tween 80 (0.010–0.21  $\mu\text{g/mL}$ ) and HPW were included as controls. All stock solutions were filtered by 0.2  $\mu\text{m}$  syringe filter. The untreated control group was cell media only. Confluent cell monolayers in 96 well microplates were treated with 150  $\mu\text{L}$  of sample in Gibco Dulbecco's modified Eagle's medium (DMEM) supplemented with 5% foetal bovine serum and 1% penicillin/streptomycin to a final volume of 300  $\mu\text{L}$  per well and incubated for 24 h at 37 °C with 5%  $\text{CO}_2$ . The microplates were then incubated with 20  $\mu\text{L}$  of 5 mg/mL MTT solution per well for 4 h at 37 °C and 5%  $\text{CO}_2$ . Following incubation, the media in each well was discarded, and 100  $\mu\text{L}$  of 10% sodium dodecyl sulphate (SDS) solution in 0.01M HCl was added to solubilise the purple-blue formazan. The absorbance was measured with an ELISA microplate reader (xMark™, BIO-RAD, Australia) at 570 nm. The cell viability percentage was calculated using:

$$\% \text{ cell viability} = \frac{\text{Absorbance}_{\text{sample}}}{\text{Absorbance}_{\text{control}}} \times 100 \quad (3)$$

where  $\text{absorbance}_{\text{control}}$  is the absorbance of untreated cells and  $\text{absorbance}_{\text{sample}}$  is the absorbance of treated cells with samples. Each sample and control were tested in triplicate in three independent experiments.

## The Antioxidant Activity Assay

The antioxidative capacity comparison of CTNE, TSWE and CSO was evaluated using the stable DPPH radical method demonstrated in our previous study.<sup>11</sup> Fifty microliters of CTNE, TSWE or CSO in methanol over the range of 15.6–250  $\mu\text{g/mL}$  were added to 5 mL of a 0.04% methanol solution of DPPH. Butylated hydroxytoluene (BHT)—an antioxidative substance commonly used in antioxidant activity assays—was used as a positive control in this assay. Each test was carried out in triplicate in three independent experiments. Free radical scavenging indicated by reduced DPPH in percentage was calculated as follows:

$$\text{Total antioxidant activity \%} = \frac{\text{Abs control} - \text{Abs sample}}{\text{Abs control}} \times 100 \quad (4)$$

## Evaluation of the in vitro Wound Healing Activity

The wound healing activity of CTNE, TSWE and CSO was assessed using the scratch-wound assay.<sup>34</sup> The BSR cells were seeded at a density of  $1 \times 10^5$  onto 4-well chamber slides and cultured in DMEM) supplemented with 5% foetal bovine serum and 1% penicillin/streptomycin incubated overnight at 37°C with 5%  $\text{CO}_2$ . After 72 h incubation, scratches were introduced into the confluent monolayer with a sterile 10  $\mu\text{L}$  pipette tip, and the plate was washed with PBS (Sigma Aldrich, Australia). Cells were treated by adding 150  $\mu\text{L}$  of CTNE, TSWE or CSO with supplemented DMEM to each well in a final volume of 300  $\mu\text{L}$ . The concentration of CTNE, TSWE or CSO (8.75  $\mu\text{g/mL}$ , 4.38  $\mu\text{g/mL}$ , and 2.19  $\mu\text{g/mL}$ ) was selected based on higher than 80% cell viability. Controls included untreated cells (distilled water added to media) and treatment with Fibroblast Growth Factors (FGF) (Sigma Aldrich, Germany) at a final concentration of 2ng/

mL. To evaluate the relative cell migration for each treatment, three locations of the scratch-wound from each chamber were photographed and measured using an OLYMPUS DP22 Microscope Digital Camera. In order to measure the scratch gap area at 0 h, 24 h and 48 h, DP2-SAL Software was used to determine the percentage of wound closure at each time point. Three independent experiments were performed with triplicates, the data were recorded, and wound closure percentages were calculated as follows:

$$\text{Wound Closure \%} = \left[ \frac{A_{T=0h} - A_{T=\Delta h}}{A_{T=0h}} \right] \times 100 \quad (5)$$

where,  $A_{T=0h}$  is the distance of wound measured immediately after scratching made and  $A_{T=\Delta h}$  is the distance of wound measured  $h$  hours after scratching made.

## Stability Study of CTNE

Freshly prepared samples were placed in 15 mL falcon tubes and stored in a refrigerator at  $4 \pm 1$  °C and room temperature of  $25 \pm 1$  °C for four weeks of storage. Samples were centrifuged at 4500 rpm for 15 min then observed for layer separation and sedimentation. The particle size and PDI values were analysed before and after four weeks of storage.

## Statistical Analysis

NE formulation, graphical representations, and optimisation were statistically analysed using Design Expert (version 12.0.3.0) software. The best-fitting polynomial model was compared by numerous statistical parameters (lack-of-fit, predicted and adjusted multiple correlation coefficients and coefficient of variation) of different polynomial models. The significant difference was determined through analysis of variance by calculating F-value at the probability of 0.5, 0.1 and 0.01.

The data obtained from cell viability, DPPH, and in vitro wound healing assays were analysed using GraphPad software (USA). The data presented are the mean  $\pm 2$  SD of three independent experiments. Statistical significance was determined using a two-way ANOVA with a P value of less than 0.05 as statistically significant.

## Results

### Liquid Chromatography–Mass Spectrometry Analysis of TSWE

The water-soluble compounds in TSWE were identified by QTOF-LC/MS (Figure 1 and Table 2). The polyphenolic-rich fractions obtained from TSWE included K-Hex-Hex\*Di-C,C-hexosyl-apigenin, Kaempferol-C-glucoside, Diosmetin 6.8-di-C-glucoside, MQ-Hex-dHx\*Isovitexin 6-O-deoxyhexoside, and Diosmetin-6-C-glucoside (\*: Q, quercetin; M, methyl; MQ, methylquercetin; MK, methylkaempferol; Hex, hexose; dHx, deoxyhexose). These components were identified by matching the retention time and chromatogram to previous publications describing these plants' extract phenolic compounds.<sup>35–38</sup>

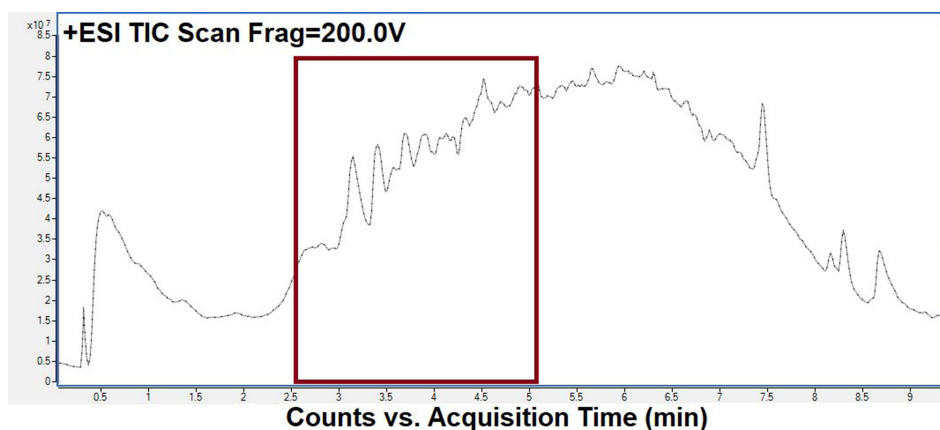


**Figure 1** Liquid chromatography–mass spectrometry (LC-MS) chromatogram of *Tinospora smilacina* leaf water extract.

**Table 2** Liquid Chromatography–Mass Spectrometry (LC-MS) Identification of Compounds in *Tinospora smilacina* Leaf Water Extract

Compound	Retention Time (min)	Molecular Mass	Empirical Formula	References
K-Hex-Hex*	2.49	610	C <sub>27</sub> H <sub>30</sub> O <sub>16</sub>	[35]
Di-C,C-hexosyl-apigenin	3.04	594	C <sub>30</sub> H <sub>26</sub> O <sub>13</sub>	[36]
Kaempferol-C-glucoside	3.83	448	C <sub>21</sub> H <sub>20</sub> O <sub>11</sub>	[37]
Diosmetin 6,8-di-C-glucoside	3.616	624	C <sub>28</sub> H <sub>32</sub> O <sub>16</sub>	[38]
MQ-Hex-dHx*	3.91	624	-	[35]
Isovitexin 6-O-deoxyhexoside	4.43	578	C <sub>27</sub> H <sub>29</sub> O <sub>14</sub>	[39]
Diosmetin-6-C-glucoside	4.51	462	C <sub>22</sub> H <sub>22</sub> O <sub>11</sub>	[38]

**Abbreviations:** \*Q, quercetin; M, methyl; MQ, methylquercetin; MK, methylkaempferol; Hex, hexose; dHx, deoxyhexose.

## Optimisation of CTNE Using D-Optimal Mixture Design

The mixture components and process factor values used in DMD are presented in Table 3. The experimental design model was quadratic (Equation S1 and S2 shown in Supplementary Material). The mixture components are interconnected as they are compelled to sum one, though the procedure variables can be altered independently. The factor valuation and the corresponding droplet size and PDI values revealed that three independent variables, CSO (A), Tween 80 (B) and TSWE: HPW (C), had a significant consequence on the encapsulation of NEs ( $P < 0.05$ ).

The mixture components were prepared by using diverse levels of independent variables. Details regarding the effect of independent variables on response variables and statistical analysis of the models are summarised in Supplementary Material. The response surface plots for droplet size and PDI value are presented in Figure 2. The effect of factors on the droplet size and the PDI value could be understood by analysing the elevation of the corresponding response surface. A higher elevation corresponds to large droplet size and PDI value and vice versa.

The optimum CTNE values were 7% CSO, 21% Tween 80, and 72% TSWE: HPW, which resulted in particles with a size of 21.87 nm and a PDI value of 0.19. The visual appearance of CTNE is presented in Figure 3a.

## TEM Observation of CTNE Droplets

The morphology of CTNE was imaged by TEM (Figures 3b and c). The TEM observations provided positive images in which the CTNE appeared as bright and spherical shapes with dark surroundings. The CTNE particles were distributed uniformly and homogeneously throughout the formulation without any aggregation in the system. Moreover, the average droplet size obtained from the TEM image was approximately  $24 \pm 5$  nm and agreed with the particle size analysis results using the Zetasizer analysis.

**Table 3** Mixture Components and Process Factor Values Used in D-Optimal Mixture Design (DMD)

Run	A: CSO %	B: Tween 80%	C: TSWE: HPW %	Droplet Size (nm)	Polydispersity Index
1	8.0	18.7	73.3	112.67	0.65
2	8.0	22.4	69.6	60.35	0.35
3	6.7	18.0	75.3	63.02	0.31
4	6.7	18.0	75.3	60.67	0.36
5	6.3	24.0	69.6	20.11	0.19
6	6.0	21.5	72.5	22.15	0.31
7	7.2	21.3	71.5	23.49	0.19
8	6.0	20.3	73.7	31.41	0.37
9	6.0	22.8	71.2	21.53	0.24
10	6.9	19.0	74.2	45.63	0.25
11	7.2	21.3	71.5	23.33	0.21
12	8.0	24.0	68.0	40.47	0.24
13	7.2	21.3	71.5	23.08	0.21
14	7.6	20.0	72.4	56.63	0.31

**Abbreviations:** CSO, *Calophyllum inophyllum* seed oil; HPW, high pure water; TSWE, *Tinospora smilacina* water extract.

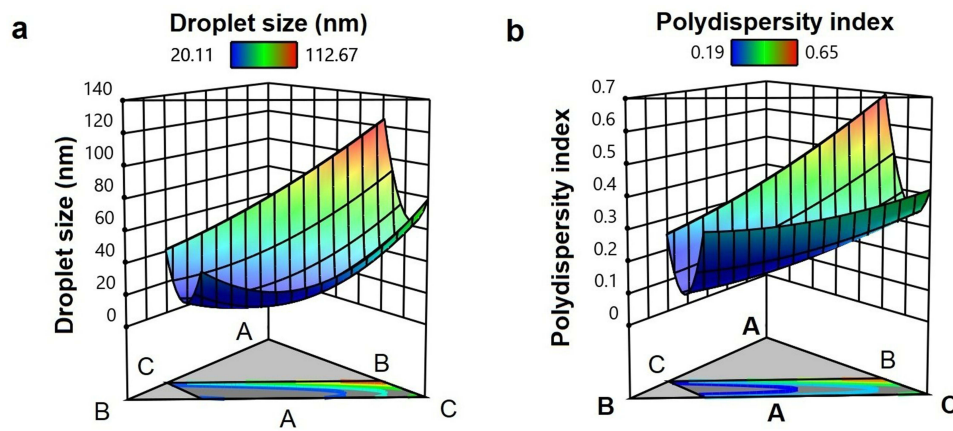


**Figure 2** Three-dimensional response surface plot representing the effect of (A) *Calophyllum inophyllum* seed oil (CSO) (%), (B) Tween 80 (%) and (C) *Tinospora smilacina* water extract: high pure water (TSWE: HPW) (%) on (a) droplet size (nm) and (b) polydispersity index.

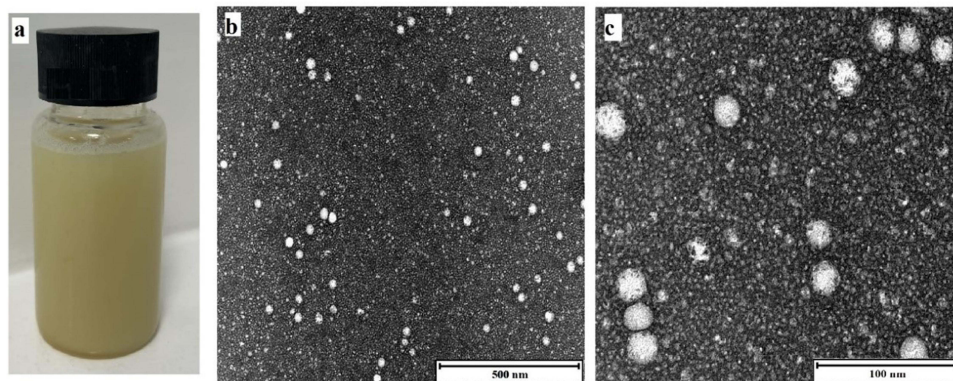


**Figure 3** (a) Illustration of *Tinospora smilacina* water extract and *Calophyllum inophyllum* seed oil nanoemulsion (CTNE), (b and c) transmission electron microscopy of droplets in the CTNE. Scale bar (b) 500 nm and (c) 100 nm.

### Stability Study of CTNE

After four weeks of storage, the droplet size and phase separation were tested to evaluate physical stability. The optimised NE sample was physically stable with no phase separation at room temperature and 2–8 °C. The particle size and PDI values were also compared before and after four weeks of storage (Table 4). This indicated refrigeration was the best storage method for CTNE with no droplet size or PDI change over four weeks.

### Cell Viability Assay

The MTT assay used to examine the effect of CTNE, TSWE and CSO on the viability of the BSR cell line is present in Figure 4. The CTNE, TSWE and CSO were tested over a range of concentrations from 60–4000 µg/mL. The untreated

**Table 4** Stability of *Tinospora smilacina* Water Extract and *Calophyllum inophyllum* Seed Oil NE (CTNE), After Four Weeks of Storage at Different Temperature

	At Preparation	Four Weeks of Storage	
		Room Temperature	Refrigeration
<b>Droplet Size (nm)</b>	24 ± 5	44 ± 5	24 ± 5
<b>Polydispersity index</b>	0.21 ± 0.02	0.24 ± 0.02	0.21 ± 0.02

**Note:** Each value is the mean of three replicates with standard deviation (±2 SD) and analysed by 2-way-ANOVA (analysis of variance) (n = 3).

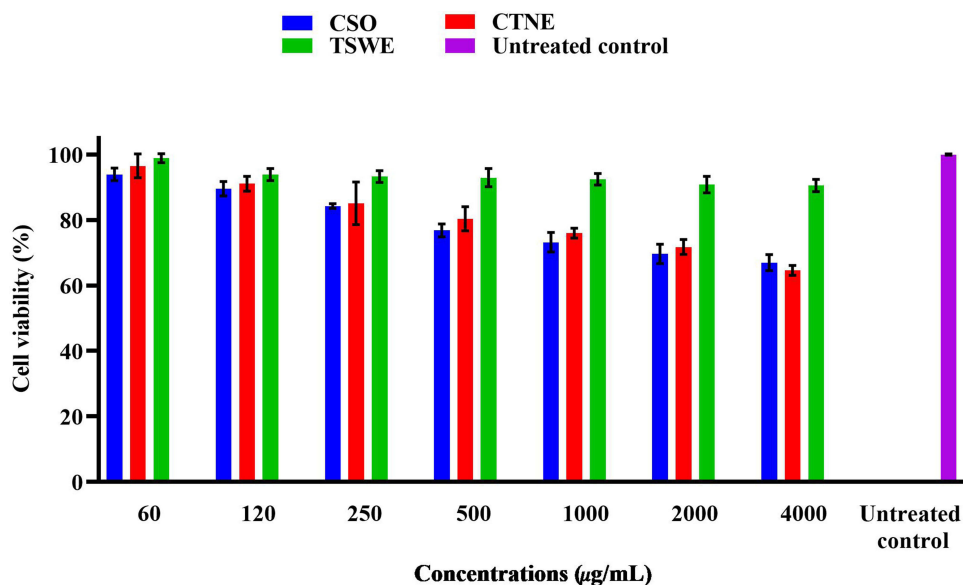


**Figure 4** Cell Viability profile by MTT assay of *Calophyllum inophyllum* seed oil (CSO), *Tinospora smilacina* water extract (TSWE) and CSO nanoemulsion (CTNE) and TSWE at 24 h on hamster kidney (BSR) cell line. The x-axis indicates the NE concentration matched with the equivalent TSWE and CSO concentration content available in NE. The untreated control contained cells with media only. Each value is the mean of three replicates with standard deviation ( $\pm 2$  SD) and all conditions were significantly different to the untreated control analysed by two-way-ANOVA ( $n = 3$ ;  $p < 0.05$ ).

control treated with media only was set as 100% cell viability. The TSWE showed more than 90% cell viability at all concentrations tested. The CSO and CTNE significantly ( $p < 0.0001$ ) affected cell viability at 1000  $\mu\text{g/mL}$  and greater, and the cell viability dropped to less than 80%. The cell viability in CTNE was consistently higher than CSO, except at the highest concentration tested of 4000  $\mu\text{g/mL}$ . CTNE presented above 80% cell viability when the concentration was less than 500  $\mu\text{g/mL}$  or less. The CSO showed cell viability above 80% at less than 250  $\mu\text{g/mL}$  or less. The CTNE and TSWE in 60  $\mu\text{g/mL}$  were not significantly different from the untreated control group. The three lowest concentrations tested of CTNE, TSWE and CSO were used in wound healing experiments as they showed above 250  $\mu\text{g/mL}$  (~85%), 120  $\mu\text{g/mL}$  (~90%) and 60  $\mu\text{g/mL}$  (~95%) cell viability. An equivalent amount of Tween 80 present in the NE was also examined for its effect on cell viability and showed above 80% cell viability (data not shown in Figure 4).

## Free Radical Scavenging of CTNE, TSWE and CSO

The DPPH free radical scavenging abilities of CTNE, TSWE and CSO are shown in Figure 5. The antioxidant activity of all tested samples was concentration dependent. The CTNE demonstrated the highest levels of activity, while the TSWE showed higher radical scavenging in all tested concentrations when compared to CSO. At the highest concentration of CTNE, TSWE and CSO (250  $\mu\text{g/mL}$ ), 30%, 25% and 15% of free radicals were quenched, respectively. These results were significantly different ( $p < 0.0001$ ).

## Evaluation of the Wound Healing Effect of CTNE, TSWE and CSO

The effect of CTNE, TSWE and CSO on wound closure (WC) were assessed using a monolayer scratch model. Three concentrations of CTNE, TSWE or CSO were tested. Figure 6a displays the percentage WCs at 24 h and 48 h, while Figure 6b indicates the relative concentration of the components available in CTNE. The FGF treatment showed similar wound closure percentage (WC%) to untreated cells at 24 h and complete closure after 48 h compared to 70% WC for untreated cells. The WC% for CTNE-treated cells was consistently higher than that for FGF-treated cells. For CTNE and CSO, the WC% was most significant in the cells treated with the lowest concentration ( $p < 0.0001$ ). This contrasted with TSWE treatment, which demonstrated similar levels of wound closure at all tested concentrations. The WC% for all TSWE concentrations was higher than that for FGF treatment at 24 h. However, complete WC was not achieved at 48 h for TSWE and only reached a maximum of 72%.

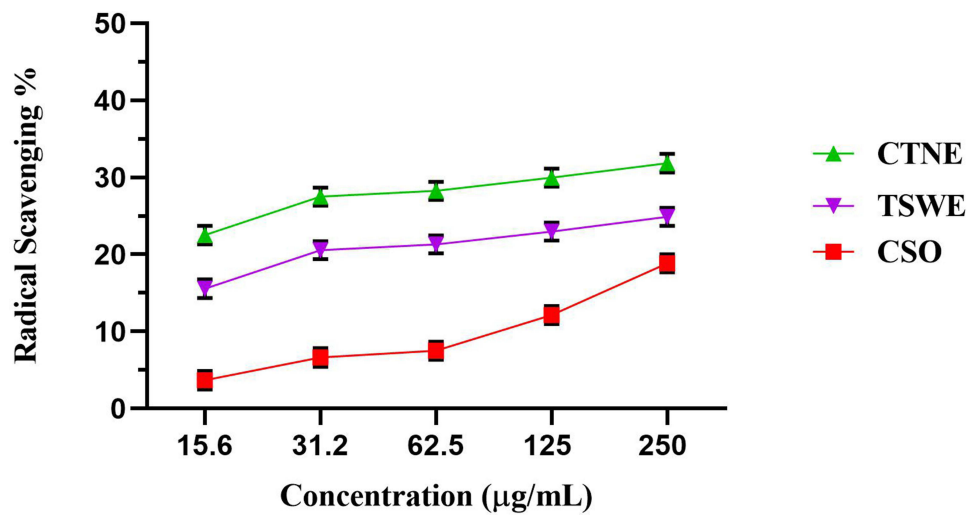
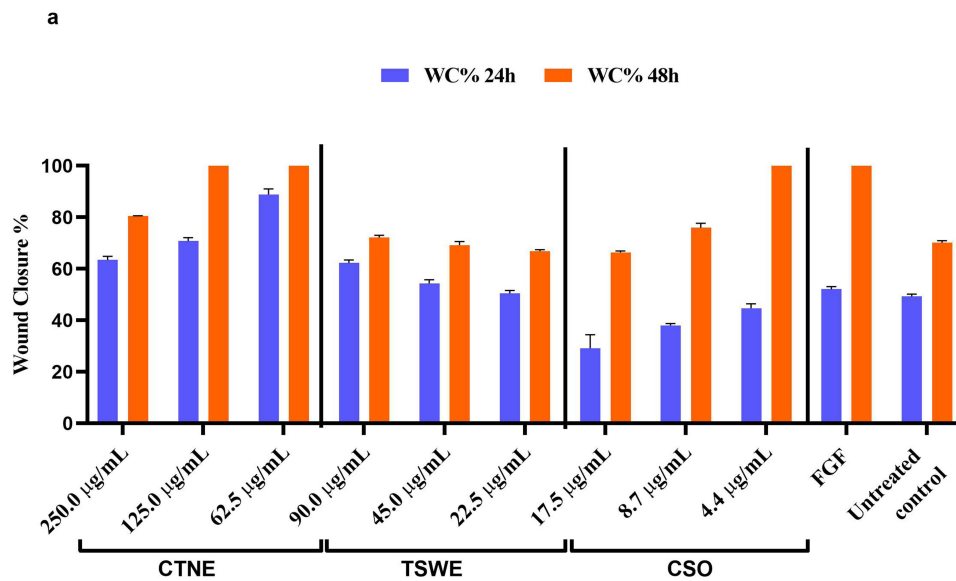


**Figure 5** DPPH radical scavenging of *Calophyllum inophyllum* seed oil (CSO), *Tinospora smilacina* water extract (TSWE) and CSO nanoemulsion (CTNE) and TSWE. The DPPH results are the mean of three independent experiments with error bars  $\pm 2SD$ . The x-axis indicates the NE concentration matched with the equivalent TSWE and CSO concentrations available in NE.



b

CTNE (µg/mL)	Relative concentration of components	
	TSWE(µg/mL)	CSO(µg/mL)
250.00	90.00	17.50
125.00	45.00	8.75
62.50	22.50	4.38

**Figure 6 (a)** Percentage wound closure observed for *Calophyllum inophyllum* seed oil (CSO), *Tinospora smilacina* water extract (TSWE) and CSO nanoemulsion (CTNE) and TSWE at 24 h and 48 h in hamster kidney (BSR) cells. Blank indicates untreated cells (negative control), FGF indicates Fibroblast Growth Factor (positive control) and cells with media only negative control. Each value is the mean of three individual experiments with standard deviation ( $\pm 2SD$ ) and analysed by two-way analysis of variance (ANOVA) ( $n = 3$ ;  $p < 0.0001$ ). **(b)** Relative concentration of components available in CTNE.

Figure 7 displays a typical image of the wound closure at the lowest concentration of CTNE, CSO and TWSE treatments at 0 h, 24 h, and 48 h. Cells treated with the lowest concentration of CTNE (62.5  $\mu\text{g}/\text{mL}$ ) achieved 90% WC in 24 h and complete WC in 48 h. This was higher than all other treatments, including FGF-treated cells at 24 h (52%

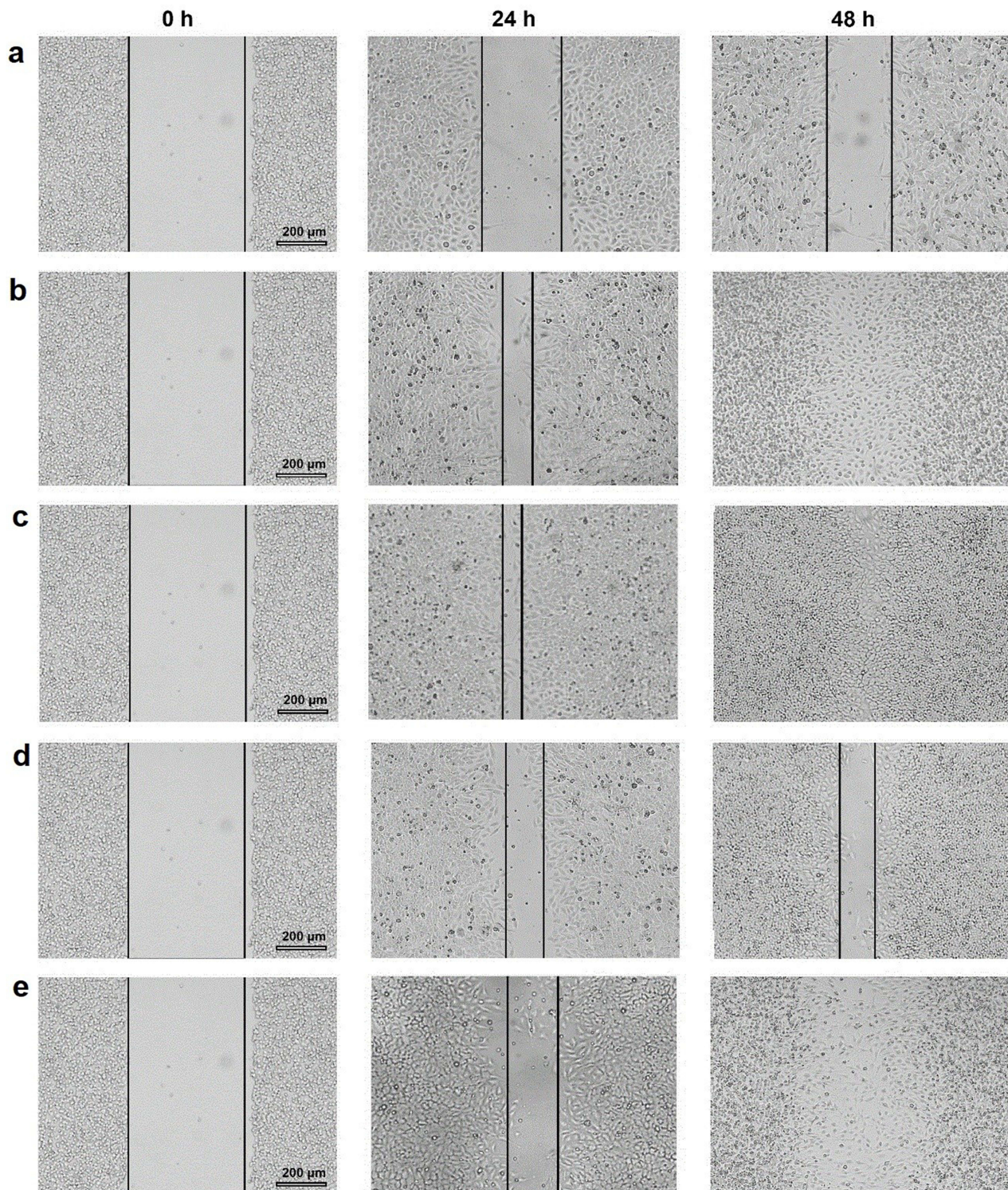


**Figure 7** Wound closure photomicrograph of *Calophyllum inophyllum* seed oil (CSO), *Tinospora smilacina* water extract (TSWE) and CSO nanoemulsion (CTNE) and TSWE at 24 h and 48 h in hamster kidney (BSR) cells. (a) Untreated control. (b) Fibroblast growth factors (FGF; positive control). (c) CTNE:62.5  $\mu\text{g}/\text{mL}$ . (d) TSWE:22.5  $\mu\text{g}/\text{mL}$ . (e) CSO: 4.3  $\mu\text{g}/\text{mL}$ . Black solid lines represent the wound size ( $\mu\text{m}$ ) of the BSR cell line monolayer.

WC). The lowest concentration of CSO treatment (4.38  $\mu\text{g/mL}$ ) displayed 46% WC after 24 h and reached 100% WC after 48 h. The untreated control group indicates the cells' natural migration rate without the influence of any samples or growth factors.

## Discussion

In this study we produced NE combining *T. smilacina* and *C. inophyllum*, in order to integrate the bioactive compounds of both native plants in a single formulation. The stable NE was characterised in comparison to the native plant components. During this process, flavonoid compounds were identified in the TSWE. Seven flavonoids were identified by comparing the retention time and chromatogram with previous studies on plant extract flavonoids.<sup>35–41</sup> A limitation of this study was that the commercial standards were not used for identification due to financial restrictions. However, retention time was a standard method for identifying compounds.<sup>42</sup> Some of the flavonoids identified in this study have previously been isolated and identified from the stems of *T. smilacina* including columbin, isolariciresinol, dihydrosyringenin, jateorin, palmatoside F, and menispermacide.<sup>43</sup> In addition, the biomedical properties of some of these flavonoid compounds, extracted from different plant materials, have been described by previous studies.<sup>44</sup> For example, the diosmetin 6,8-di-C-glucoside identified in TSWE is a flavonoid found in other medicinal herbs, such as oregano and citrus.<sup>45,46</sup> Previous studies on diosmetin's effects reported anti-cancer, anti-inflammatory, and anti-atopic properties.<sup>47–49</sup> Two of the other flavonoid compounds identified in TSWE have been shown to competitively limit tyrosinase activity through their ability to chelate metal, resulting in irreversible enzyme inactivation.<sup>50,51</sup> Tyrosinase is a commonly available copper-containing enzyme that is required for the production of melanin, the biopolymer that provides colours for the skin and hair, as well as protects skin from ultraviolet radiation.<sup>50</sup> Thus, the presence of bioactive compounds in TSWE with potential skin benefits improved the activity of the CTNE.

This study found that D-optimal mixture design and RSM were suitable for describing the interaction between mixture components and the optimisation of CTNE formulation. Mixture design is one of the most useful statistical techniques to optimise the ingredients found in the formula.<sup>52,53</sup> The response surface models explained more than 90% of the variation in the response variables studied as a function of the main emulsion components.<sup>25</sup> The optimum experimental values determined by this study corresponded well with the predicted droplet size and PDI value ([Figure S1](#)). Based on ANOVA results, the proximity of  $R^2$  (0.9513) to unity demonstrated that the influence of CSO (A), Tween 80 (B) and TSWE: HPW (C) on response variables could be adequately described through a quadratic polynomial model ([Table S1](#)). The D-optimal mixture design model in this study was similar to that found in previous studies on the optimisation NEs in the food<sup>54,55</sup> and therapeutic<sup>56,57</sup> industries. The importance of a polynomial equation's regression coefficients was frequently examined by P-values.<sup>58</sup> Here, the models obtained for responses, droplet size, and PDI were subject to ANOVA, wherein significant p-values proved the fitness of the models ( $< 0.05$ ), the non-significant lack of fit (droplet size = 0.0875, PDI = 0.2015) and high value of  $R^2$  (droplet size = 0.9971, PDI = 0.9513) ([Table S1](#)). The lack of fit was non-significant ( $p \leq 0.05$ ) relative to pure error for all variables, which indicates that our model was statistically accurate.

In this study, mean droplet size optimisation was carried out to develop the optimal NE composition with the smallest droplet size. The mean droplet size is one of the most critical characteristics of emulsions, considering it defines its type (microemulsion or nanoemulsion), and properties, including the optical stability and viscosity properties.<sup>59</sup> The prepared emulsions were defined as NEs since the mean droplet size was under 200 nm. At the lower concentration of CSO, surfactant molecules were enough to cover the oil droplets and reduce interfacial tension at the o/w interface. As such, CTNE droplet size increased at a higher level of CSO. This increase in the droplet size was due to insufficient emulsifiers to cover newly developed droplets, which begin coagulation. It has been reported that coagulation decreased once the surfactant concentration increased.<sup>60</sup> Moreover, it has been determined that emulsions with large droplets are more prone to gravity separation/creaming, and high entrapment efficiency of droplets can occur when particle sizes are small.<sup>5,61</sup> This study found that no phase separation during storage and centrifugation, indicating that formulated NE sustained stability analyses.<sup>62</sup>

Another parameter indicative of a homogenous NE system is a low PDI value. During optimisation, the PDI was between 0.19–0.65. The highest PDI value was observed when the Tween 80 to CSO ratio was 2.5%. However, by

increasing the Tween 80 concentration to 21.3%, the PDI value decreased to 0.19. The presence of the unsaturated non-polar tails of the Tween 80 allowed for their molecular packing and free creation of ultrafine droplets at the oil-water interface of CTNE, as previously reported by a similar study that used Tween 80.<sup>63</sup> The value of PDI should be as low as possible, preferably between 0.10–0.25, to describe a narrow size distribution in the system.<sup>5</sup>

We have previously formulated a NE containing CSO (CSONE). The CSONE was stable and enhanced in biomedical tests such as antioxidant activity, cell viability, in vitro wound healing, and antimicrobial activity, compared to the CSO.<sup>11</sup> In the current investigation, we introduced a plant-based water component to the NE in an effort to enhance the properties of the plant-based oil NE. When a single compound is added to the o/w NE formulation, it can attach to the outer layer of NE or be contained in the oil core, depending on its hydrophilic or lipophilic structure.<sup>64</sup> In our study, the phenolic compounds present in TSWE could attach to the hydrophilic head of surfactant or be encapsulated in the NE oil phase core.<sup>65,66</sup> For instance, curcumin is a phenolic compound that is a relatively hydrophobic molecule. A study on encapsulation of curcumin in NE formulation demonstrated that the curcumin was entrapped in the core area of NE.<sup>67</sup> When comparing TEM images of CTNE and CSONE,<sup>11</sup> some dark spots are attached to the edge of CTNE micelles which might be phenolic compounds (Figure S2), compared with the smooth droplet surface seen in CSONE. While the TEM provides valuable information on synthesised particle sizes and shapes, it is limited to the morphological appearance rather than the inner structure of NEs due to the low contrast of the NE components.

The bioactivity of CTNE was examined for antioxidant activity, cell viability and in vitro wound healing activity, and the results compared to those of TSWE and CSO. The CTNE demonstrated higher antioxidant activity than TSWE and CSO, indicating that the formulation did not inhibit the antioxidant activity contained in CSO and TSWE. Also, this activity was increased in CTNE compared to the CSONE (Figure S3). Both TSWE and CSO contain compounds with the potential for antioxidant activity. Flavonoids in TSWE, such as kaempferol-C-glucoside, are high in reducing reactive oxygen species and other oxidative stresses.<sup>68,69</sup> In CSO, oleanolic acid, a triterpenoid compound, is known to act as a potent antioxidant.<sup>70</sup> In these complex plant extracts, there may be other contributing compounds. Also, NE formulation would act to reduce droplet size and concordantly increase the specific surface area of CSO. This physical transformation could increase efficient free radical absorption. Our results support the probability of using CTNE as a natural antioxidant agent.

The MTT cell viability assay was used to confirm the absence of cytotoxic effects on mammalian cells and was compared for CTNE, TSWE and CSO. The cell viability in the presence of TSWE was consistently higher than 90%. The CSO and CTNE adversely affected cell viability (62–95%) in a concentration-dependent manner. The cell viability in the presence of CTNE was consistently but slightly higher than CSO. This may have been due to the presence of TSWE in NEs, or the nanostructure, which has been reported to affect cell viability based on size and cell type.<sup>71</sup>

Despite a small decrease in cell viability, significant wound healing activity was observed for CTNE. Cell viability is a critical aspect of controlling the proliferation and migration of the cells during the wound healing process.<sup>72,73</sup> Thus, based on the cell viability results, CTNE was used at the lowest concentrations in subsequent wound healing tests. At the most effective concentration, CTNE resulted in almost complete WC at 24 h, which significantly improved compared to the FGF-treated control ( $p > 0.0001$ ). Both the combination of NE components and NE formulation are proposed to have a role in this activity. From our previous study, the formulation of CSO as a NE increased wound healing efficacy compared to CSO in the BSR cell line.<sup>11</sup> While the effect of CSONE and CTNE have not been directly compared, the same methodology was used for both studies. The %WC for CSONE appears similar to that of CTNE, presented here, with significant WC at 24 h and complete WC at 48 h.<sup>11</sup> The potential role of TSWE in the increasing WC activity of CTNE compared to CSONE<sup>11</sup> could be due to the availability of flavonoid compounds such as kaempferol, which have previously been suggested to play a role in wound healing.<sup>74</sup> By comparing the WC in CSONE and CTNE after 48 h, the cell migration and density showed an improvement in the CTNE-treated cell group (Figure S4). This investigation of the effect on wound healing was limited to the WC assay using a non-human mammalian fibroblast cell line (BSR),<sup>32</sup> It is, however, commonly used in such work<sup>75,76</sup> and suggests further characterisation of relevant human fibroblasts and suitable models could be warranted.

## Conclusion

In this study, the preparation of CTNE using a high-shear homogenisation technique to obtain stable NE was conducted. This study illustrated RSM as a valuable tool for optimising the cooperative condition of NE and determining the relationship between mixture components (CSO, Tween 80 and TSWE: HPW) and two responses (droplet size and PDI value). The current study also shows that the D-optimal mixture design effectively described and predicted a stable NE fulfilling the  $24 \pm 5$  nm particle size and PDI value of  $0.21 \pm 0.02$ . The CTNE was stable, and its size and features remained stable after storage. An optimised CTNE formulation was used for the biological investigation. The formulation as a NE had higher antioxidant activity than NE components (CSO and TSWE) by themselves. This activity was also higher in CTNE compared to the CSONE. Similarly, CTNE has a greater cell viability effect than NE components after interaction with BSR cells. Likewise, the in vitro wound healing assay revealed that CTNE in the lowest concentrations was the most effective. Approximately 90% WC was observed in 24 h, which was greater than the FGF group and showed complete closure in 48 h. When the WC in CSONE and CTNE were compared after 48 h, the cell migration and density improved in the CTNE-treated cell group. This study has demonstrated an innovative approach to enhancing the properties of plant-based oil NEs by incorporating a plant-based water component. The resulting combination of water and oil extracts, CTNE, exhibits promising potential as stable and bioactive NEs for various biomedical applications.

## Data Sharing Statement

The datasets used and/or analysed during the current study are available from the corresponding author upon reasonable request.

## Acknowledgments

The authors are grateful to the staff of the Berrimah Veterinary Laboratory for their assistance in cell culturing and to the Central Analytical Research Facility at Queensland University of Technology (QUT CARF) for the transmission electron microscopy imaging. The assistance provided by Jeremy Garnett of Top End Editing was greatly appreciated.

## Funding

The authors would like to acknowledge Charles Darwin University for its financial support. Charles Darwin University had no role in the design of the study and collection, analysis, and interpretation of data and in writing this manuscript.

## Disclosure

The authors report no conflicts of interest in this work.

## References

1. Bonifacio BV, Silva PB, Ramos MA, Negri KM, Bauab TM, Chorilli M. Nanotechnology-based drug delivery systems and herbal medicines: a review. *Int J Nanomedicine*. 2014;9:1–15. doi:10.2147/IJN.S52634
2. Ahmad S, Alghamdi SA. A statistical approach to optimizing concrete mixture design. *Sci World J*. 2014;2014:1–7. doi:10.1155/2014/561539
3. Zaidi Z, Lanigan SW. Skin: structure and function. In: *Dermatology in Clinical Practice*. Springer; 2010:1–15.
4. Ajazuddin SS, Saraf S. Applications of novel drug delivery system for herbal formulations. *Fitoterapia*. 2010;81(7):680–689. doi:10.1016/j.fitote.2010.05.001
5. Kakde P, Jani R, Chagediya VV. A review on nanoemulsions: a recent drug delivery tool. *J Drug Deliv Ther*. 2019;9(5):185–191. doi:10.22270/jddt.v9i5.3577
6. Roberts MS, Mohammed Y, Pastore MN, et al. Topical and cutaneous delivery using nanosystems. *J Control Release*. 2017;247:86–105. doi:10.1016/j.jconrel.2016.12.022
7. Gupta M, Agrawal U, Vyas SP. Nanocarrier-based topical drug delivery for the treatment of skin diseases. *Expert Opin Drug Deliv*. 2012;9(7):783–804. doi:10.1517/17425247.2012.686490
8. Rai VK, Mishra N, Yadav KS, Yadav NP. Nanoemulsion as pharmaceutical carrier for dermal and transdermal drug delivery: formulation development, stability issues, basic considerations and applications. *J Control Release*. 2018;270:203–225. doi:10.1016/j.jconrel.2017.11.049
9. Zorzi GK, Carvalho ELS, von Poser GL, Teixeira HF. On the use of nanotechnology-based strategies for association of complex matrices from plant extracts. *Rev Bras Farmacogn*. 2015;25:426–436. doi:10.1016/j.bjp.2015.07.015
10. Atanasov AG, Zotchev SB, Dirsch VM, Supuran CT. International natural product sciences taskforce, Supuran CT: natural products in drug discovery: advances and opportunities. *Nat Rev Drug Discov*. 2021;20(3):200–216. doi:10.1038/s41573-020-00114-z

11. Saki E, Murthy V, Khandanlou R, Wang H, Wapling J, Weir R. Optimisation of Calophyllum inophyllum seed oil nanoemulsion as a potential wound healing agent. *BMC Complementary Med Ther.* 2022;22(1):1–15. doi:10.1186/s12906-022-03751-6
12. Chi S, She G, Han D, Wang W, Liu Z, Liu B. Genus tinospora: ethnopharmacology, phytochemistry, and pharmacology. *Evid Based Complementary Altern Med.* 2016;2016:1–32. doi:10.1155/2016/9232593
13. Pathak AK, Jain DC, Sharma RP. Chemistry and Biological activities of the genera tinospora. *Int J Pharmacogn.* 2008;33(4):277–287. doi:10.3109/13880209509065379
14. Aboriginal Communities of the Northern Territory. *Traditional Aboriginal Medicines in the Northern Territory of Australia.* Darwin: Conservation Commission of the Northern Territory of Australia; 1993.
15. Knight T, Barr A, Andrews M, Alexander V; Aboriginal Communities of the Northern Territory of Australia. *Traditional Bush Medicines: An Aboriginal Pharmacopoeia.* Richmond, Vic.: Greenhouse Publications; 1988.
16. Li RW, Leach DN, Myers SP, et al. Anti-inflammatory activity, cytotoxicity and active compounds of *Tinospora smilacina* Benth. *Phytother Res.* 2004;18(1):78–83. doi:10.1002/ptr.1373
17. Uzor PF. Alkaloids from plants with antimalarial activity: a review of recent studies. *Evid Based Complementary Altern Med.* 2020;2020:8749083. doi:10.1155/2020/8749083
18. Chingwaru C, Bagar T, Maroyi A, Kapewangolo PT, Chingwaru W. Wound healing potential of selected Southern African medicinal plants: a review. *J Herb Med.* 2019;17:100263. doi:10.1016/j.hermed.2019.100263
19. Li YZ, Li ZL, Yin SL, et al. Triterpenoids from *Calophyllum inophyllum* and their growth inhibitory effects on human leukemia HL-60 cells. *Fitoterapia.* 2010;81(6):586–589. doi:10.1016/j.fitote.2010.02.005
20. Sundur S, Shrivastava B, Sharma P, Raj SS, Jayasekhar VL. A review article of pharmacological activities and biological importance of *Calophyllum inophyllum*. *Int J Adv Res.* 2014;2(12):599–603.
21. Spino C, Dodier M, Sotheeswaran S. Anti-HIV coumarins from *Calophyllum* seed oil. *Bioorg Med Chem Lett.* 1998;8(24):3475–3478. doi:10.1016/S0960-894X(98)00628-3
22. Pawar KD, Joshi SP, Bhide SR, Thengane SR. Pattern of anti-HIV dipyrano coumarin expression in callus cultures of *Calophyllum inophyllum* Linn. *J Biotechnol.* 2007;130(4):346–353. doi:10.1016/j.jbiotec.2007.04.024
23. Souza Mdo C, Beserra AM, Martins DC, et al. In vitro and in vivo anti-Helicobacter pylori activity of *Calophyllum brasiliense* Camb. *J Ethnopharmacol.* 2009;123(3):452–458. doi:10.1016/j.jep.2009.03.030
24. Morel C, Séraphin D, Oger J-M, et al. New Xanthenes from *Calophyllum caledonicum*. *J Nat Prod.* 2000;63(11):1471–1474. doi:10.1021/np000215m
25. Chelladurai SJS, Murugan K, Ray AP, Upadhyaya M, Narasimharaj V, Gnanasekaran S. Optimization of process parameters using response surface methodology: a review. *Mater Today.* 2021;37:1301–1304.
26. Li Z, Lu D, Gao X. Optimization of mixture proportions by statistical experimental design using response surface method: a review. *J Build Eng.* 2021;36:102101. doi:10.1016/j.jobee.2020.102101
27. Mohamad Zen NI, Abd Gani SS, Shamsudin R, Fard Masoumi HR. The use of D-optimal mixture design in optimizing development of okara tablet formulation as a dietary supplement. *Sci World J.* 2015;2015:1–7. doi:10.1155/2015/684319
28. Parikh K, Mundada P, Sawant K. Design and optimization of controlled release felbamate tablets by d-optimal mixture design: in vitro-in vivo evaluation. *Indian J Pharm Sci.* 2019;81(1):71–81. doi:10.4172/pharmaceutical-sciences.1000481
29. Eriksson L, Johansson E, Kettaneh-Wold N, Wikström C, Wold S. *Design of Experiments, Principles and Applications.* Umetrics AB; 2000.
30. Esbensen KH, Guyot D, Westad F, Houmoller LP. *Multivariate Data Analysis: In Practice: An Introduction to Multivariate Data Analysis and Experimental Design.* Multivariate Data Analysis; 2002.
31. Vater C, Hlawaty V, Werdenits P, et al. Effects of lecithin-based nanoemulsions on skin: short-time cytotoxicity MTT and BrdU studies, skin penetration of surfactants and additives and the delivery of curcumin. *Int J Pharm.* 2020;580:119209. doi:10.1016/j.ijpharm.2020.119209
32. Buchholz UJ, Finke S, Conzelmann -K-K. Generation of bovine respiratory syncytial virus (BRSV) from cDNA: BRSV NS2 is not essential for virus replication in tissue culture, and the human RSV leader region acts as a functional BRSV genome promoter. *J Virol.* 1999;73(1):251–259. doi:10.1128/JVI.73.1.251-259.1999
33. Bopage NS, Kamal Bandara Gunaherath GM, Jayawardena KH, Wijeyaratne SC, Abeysekera AM, Somaratne S. Dual function of active constituents from bark of *Ficus racemosa* L in wound healing. *BMC Complement Altern Med.* 2018;18(1):29. doi:10.1186/s12906-018-2089-9
34. Shanmugapriya K, Kim H, Saravana PS, Chun BS, Kang HW. Astaxanthin-alpha tocopherol nanoemulsion formulation by emulsification methods: investigation on anticancer, wound healing, and antibacterial effects. *Colloids Surf B Biointerfaces.* 2018;172:170–179. doi:10.1016/j.colsurfb.2018.08.042
35. Geng P, Zhang R, Aisa HA, et al. Fast profiling of the integral metabolism of flavonols in the active fraction of *Gossypium herbaceum* L. using liquid chromatography/multi-stage tandem mass spectrometry. *Rapid Comm Mass Spectrom.* 2007;21(12):1877–1888. doi:10.1002/rcm.3031
36. Cavaliere C, Foglia P, Pastorini E, Samperi R, Laganà A. Identification and mass spectrometric characterization of glycosylated flavonoids in *Triticum durum* plants by high-performance liquid chromatography with tandem mass spectrometry. *Rapid Comm Mass Spectrom.* 2005;19(21):3143–3158. doi:10.1002/rcm.2185
37. Hassan WHB, Abdelaziz S, Al Yousef HM. Chemical composition and biological activities of the aqueous fraction of *Parkinsonia aculeata* L. growing in Saudi Arabia. *Arab J Chem.* 2019;12(3):377–387. doi:10.1016/j.arabjc.2018.08.003
38. Brito A, Ramirez JE, Areche C, Sepúlveda B, Simirgiotis MJ. HPLC-UV-MS profiles of phenolic compounds and antioxidant activity of fruits from three citrus species consumed in Northern Chile. *Molecules.* 2014;19(11):17400–17421. doi:10.3390/molecules191117400
39. Ozarowski M, Piasecka A, Paszal-Jaworska A, et al. Comparison of bioactive compounds content in leaf extracts of *Passiflora incarnata*, *P. caerulea* and *P. alata* and in vitro cytotoxic potential on leukemia cell lines. *Rev Bras Farmacogn.* 2018;28:179–191. doi:10.1016/j.bjp.2018.01.006
40. Sharma V, Janmeda P. Extraction, isolation and identification of flavonoid from *Euphorbia neriifolia* leaves. *Arab J Chem.* 2017;10(4):509–514. doi:10.1016/j.arabjc.2014.08.019
41. Khandanlou R, Murthy V, Wang H. Gold nanoparticle-assisted enhancement in bioactive properties of Australian native plant extracts, *Tasmannia lanceolata* and *Backhousia citriodora*. *Mater Sci Eng C.* 2020;112:110922. doi:10.1016/j.msec.2020.110922

42. Cassien M, Mercier A, Thétiot-Laurent S, et al. Improving the antioxidant properties of *Calophyllum inophyllum* seed oil from French Polynesia: development and biological applications of resinous ethanol-soluble extracts. *Antioxidants*. 2021;10(2):199. doi:10.3390/antiox10020199
43. Hungerford NL, Sands DPA, Kitching W. Isolation and structure of some constituents of the Australian medicinal plant *Tinospora smilacina* ('snakevine'). *Aust J Chem*. 1998;51(12):1103–1112. doi:10.1071/C98034
44. Chang SK, Jiang Y, Yang B. An update of prenylated phenolics: food sources, chemistry and health benefits. *Trends Food Sci Technol*. 2021;108:197–213. doi:10.1016/j.tifs.2020.12.022
45. Roowi S, Crozier A. Flavonoids in tropical citrus species. *J Agric Food Chem*. 2011;59(22):12217–12225. doi:10.1021/jf203022f
46. Mueller M, Lukas B, Novak J, Simoncini T, Genazzani AR, Jungbauer A. Oregano: a source for peroxisome proliferator-activated receptor  $\gamma$  antagonists. *J Agric Food Chem*. 2008;56(24):11621–11630. doi:10.1021/jf802298w
47. Chan BCL, Ip M, Gong H, et al. Synergistic effects of diosmetin with erythromycin against ABC transporter over-expressed methicillin-resistant *Staphylococcus aureus* (MRSA) RN4220/pUL5054 and inhibition of MRSA pyruvate kinase. *Phytomedicine*. 2013;20(7):611–614. doi:10.1016/j.phymed.2013.02.007
48. Chandler D, Woldu A, Rahmadi A, et al. Effects of plant-derived polyphenols on TNF- $\alpha$  and nitric oxide production induced by advanced glycation endproducts. *Mol Nutr Food Res*. 2010;54(S2):S141–S150. doi:10.1002/mnfr.200900504
49. Lee D-H, Park J-K, Choi J, Jang H, Seol J-W. Anti-inflammatory effects of natural flavonoid diosmetin in IL-4 and LPS-induced macrophage activation and atopic dermatitis model. *Int Immunopharmacol*. 2020;89:107046. doi:10.1016/j.intimp.2020.107046
50. Kim Y-J, Uyama H. Tyrosinase inhibitors from natural and synthetic sources: structure, inhibition mechanism and perspective for the future. *Cell Mol Life Sci*. 2005;62(15):1707–1723. doi:10.1007/s00018-005-5054-y
51. Badria F, elGayyar MA. A new type of tyrosinase inhibitors from natural products as potential treatments for hyperpigmentation. *Boll Chim Farm*. 2001;140(4):267–271.
52. Yolmeh M, Jafari SM. Applications of response surface methodology in the food industry processes. *Food Bioprocess Technol*. 2017;10(3):413–433. doi:10.1007/s11947-016-1855-2
53. Buruk Sahin Y, Aktar Demirtaş E, Burnak N. Mixture design: a review of recent applications in the food industry. *Pamukkale Univ J Eng Sci*. 2016;22(4):297–304. doi:10.5505/pajes.2015.98598
54. Oluwole AO, Ikhu-Omoregbe DI, Iideani VA, Ntwampe SK. Effect of African catfish mucilage concentration on stability of nanoemulsion using d-optimal mixture design. *Appl Sci*. 2021;11(15):6672. doi:10.3390/app11156672
55. Yakoubi S, Kobayashi I, Uemura K, et al. Essential-oil-loaded nanoemulsion lipidic-phase optimization and modeling by response surface methodology (RSM): enhancement of their antimicrobial potential and bioavailability in nanoscale food delivery system. *Foods*. 2021;10(12):3149. doi:10.3390/foods10123149
56. Shukla T, Pandey SP, Khare P, Upmanyu N. Development of ketorolac tromethamine loaded microemulsion for topical delivery using D-optimal experimental approach: characterization and evaluation of analgesic and anti-inflammatory efficacy. *J Drug Deliv Sci Technol*. 2021;64:102632. doi:10.1016/j.jddst.2021.102632
57. Jusril NA, Abu Bakar SI, Khalil KA, Md Saad WM, Wen NK, Adenan MI. Development and optimization of nanoemulsion from ethanolic extract of centella asiatica (nanoSECA) using d-optimal mixture design to improve blood-brain barrier permeability. *Evid Based Complementary Altern Med*. 2022;2022:1–18. doi:10.1155/2022/3483511
58. Myers RH, Montgomery DC, Anderson-Cook CM. *Response Surface Methodology: Process and Product Optimization Using Designed Experiments*. John Wiley & Sons; 2016.
59. Hussain Z, Thu HE, Ng SF, Khan S, Katas H. Nanoencapsulation, an efficient and promising approach to maximize wound healing efficacy of curcumin: a review of new trends and state-of-the-art. *Colloids Surf B Biointerfaces*. 2017;150:223–241. doi:10.1016/j.colsurfb.2016.11.036
60. Mehmood T, Ahmed A, Ahmad A, Ahmad MS, Sandhu MA. Optimization of mixed surfactants-based beta-carotene nanoemulsions using response surface methodology: an ultrasonic homogenization approach. *Food Chem*. 2018;253:179–184. doi:10.1016/j.foodchem.2018.01.136
61. Polychniatou V, Tzia C. Evaluation of surface-active and antioxidant effect of olive oil endogenous compounds on the stabilization of water-in-olive-oil nanoemulsions. *Food Chem*. 2018;240:1146–1153. doi:10.1016/j.foodchem.2017.08.044
62. Franklyne JS, Iyer S, Ebenazer A, Mukherjee A, Chandrasekaran N. Essential oil nanoemulsions: antibacterial activity in contaminated fruit juices. *Int J Food Sci Technol*. 2019;54(9):2802–2810. doi:10.1111/ijfs.14195
63. Saberi AH, Fang Y, McClements DJ. Fabrication of vitamin E-enriched nanoemulsions: factors affecting particle size using spontaneous emulsification. *J Colloid Interface Sci*. 2013;391:95–102. doi:10.1016/j.jcis.2012.08.069
64. Jiang T, Liao W, Charcosset C. Recent advances in encapsulation of curcumin in nanoemulsions: a review of encapsulation technologies, bioaccessibility and applications. *Food Res Int*. 2020;132:109035. doi:10.1016/j.foodres.2020.109035
65. Chen L, Gnanaraj C, Arulselvan P, El-Seedi H, Teng H. A review on advanced microencapsulation technology to enhance bioavailability of phenolic compounds: based on its activity in the treatment of type 2 diabetes. *Trends Food Sci Technol*. 2019;85:149–162. doi:10.1016/j.tifs.2018.11.026
66. Tungmunthithum D, Thongboonyou A, Pholboon A, Yangsabai A. Flavonoids and other phenolic compounds from medicinal plants for pharmaceutical and medical aspects: an overview. *Medicines*. 2018;5(3):93. doi:10.3390/medicines5030093
67. Chuacharoen T, Prasongsuk S, Sabliov CM. Effect of surfactant concentrations on physicochemical properties and functionality of curcumin nanoemulsions under conditions relevant to commercial utilization. *Molecules*. 2019;24(15):2744. doi:10.3390/molecules24152744
68. Biharee A, Sharma A, Kumar A, Jaitak V. Antimicrobial flavonoids as a potential substitute for overcoming antimicrobial resistance. *Fitoterapia*. 2020;146:104720. doi:10.1016/j.fitote.2020.104720
69. Kumar S, Pandey AK. Chemistry and biological activities of flavonoids: an overview. *Sci World*. 2013;2013:162750.
70. Pawar KD, Patil RV. Phytochemicals of *Calophyllum inophyllum*. In: *Bioactive Compounds in Underutilized Fruits and Nuts*. Springer; 2020:317–327.
71. Kong B, Seog JH, Graham LM, Lee SB. Experimental considerations on the cytotoxicity of nanoparticles. *Nanomedicine*. 2011;6(5):929–941. doi:10.2217/nmm.11.77
72. Rodrigues M, Kosaric N, Bonham CA, Gurtner GC. Wound healing: a cellular perspective. *Physiol Rev*. 2019;99(1):665–706. doi:10.1152/physrev.00067.2017

73. Wiegand C, Abel M, Hipler U-C, Elsner P. Effect of non-adhering dressings on promotion of fibroblast proliferation and wound healing in vitro. *Sci Rep.* 2019;9(1):1–10.
74. Özay Y, Güzel S, Yumrutaş Ö, et al. Wound healing effect of kaempferol in diabetic and nondiabetic rats. *J Surg Res.* 2019;233:284–296. doi:10.1016/j.jss.2018.08.009
75. Yousry C, Saber MM, Abd-Elsalam WH. A cosmeceutical topical water-in-oil nanoemulsion of natural bioactives: design of experiment, *in vitro* characterization, and *in vivo* skin performance against UVB irradiation-induced skin damages. *Int J Nanomedicine.* 2022;17:2995. doi:10.2147/IJN.S363779
76. Puteri FH, Widjaja J, Cahyani F, Mooduto L, Wahjuningrum DA. The comparative toxicity of xanthenes and tannins in mangosteen (*Garcinia mangostana* Linn.) pericarp extract against BHK-21 fibroblast cell culture. *Contemp Clin Dent.* 2019;10(2):319. doi:10.4103/ccd.ccd\_579\_18

### Clinical, Cosmetic and Investigational Dermatology

Dovepress

### Publish your work in this journal

Clinical, Cosmetic and Investigational Dermatology is an international, peer-reviewed, open access, online journal that focuses on the latest clinical and experimental research in all aspects of skin disease and cosmetic interventions. This journal is indexed on CAS. The manuscript management system is completely online and includes a very quick and fair peer-review system, which is all easy to use. Visit <http://www.dovepress.com/testimonials.php> to read real quotes from published authors.

Submit your manuscript here: <https://www.dovepress.com/clinical-cosmetic-and-investigational-dermatology-journal>